

Characterization of Pulsar Sources for X-ray Navigation

Paul S. Ray, Kent S. Wood, Michael T. Wolff

Abstract The Station Explorer for X-ray Timing and Navigation Technology (SEXTANT) is a technology demonstration enhancement to the Neutron Star Interior Composition Explorer (NICER) mission, which is scheduled to launch in 2017 and will be hosted as an externally attached payload on the International Space Station (ISS). During NICER's 18-month baseline science mission to understand ultra-dense matter through observations of neutron stars in the soft X-ray band, SEXTANT will, for the first-time, demonstrate real-time, on-board X-ray pulsar navigation. Using NICER/SEXTANT as an example, we describe the factors that determine the measurement errors on pulse times of arrival, including source and background count rates, and pulse profile shapes. We then describe properties of the SEXTANT navigation pulsar catalog and prospects for growing it once NICER launches. Finally, we describe the factors affecting the prediction of pulse arrival times in advance, including variable interstellar propagation effect and red timing noise. Together, all of these factors determine how well a particular realization of an X-ray pulsar-based navigation system will perform.

1 Introduction

As described in Chapter [** Bernhardt **], X-ray emitting pulsars can be used as the basis of a spacecraft navigation system [1]. Pulsars are neutron stars formed in supernova explosions that are born with spin periods of ~ 10 ms. As they age they

Paul S. Ray
Naval Research Laboratory, Washington, DC USA e-mail: paul.ray@nrl.navy.mil

Kent S. Wood
Praxis Inc., resident at Naval Research Laboratory, Washington, DC USA e-mail: kent.wood@tsc.com

Michael T. Wolff
Naval Research Laboratory, Washington, DC USA e-mail: michael.wolff@nrl.navy.mil

spin down to periods as long as several seconds under the influence of electromagnetic torque associated with a rotating dipolar magnetic field. The torque removes rotational kinetic energy, and a fraction of this released energy loss manifests as beamed radiation produced along open field lines emanating from the polar caps. This emission, which can extend from radio frequencies to γ -rays, appears as pulses repeating at the neutron star's rotation period.

A pulsar of this type is a rotation-powered pulsar (RPP). There are other types, including accreting neutron stars and magnetars, but they are of less interest for navigation, because of their transient behavior and complex period evolution. The magnitude of rotational instabilities observed in RPPs (known as timing noise) is positively correlated with the spin period derivative [2]. Younger, more energetic, pulsars have more timing noise and this limits their navigational usefulness. The most promising class of pulsars for navigation are millisecond pulsars (MSPs). These pulsars have been spun up, gaining angular momentum through accretion of material from binary companions for prolonged periods, of order 10^8 years. During this phase, the torque associated with accretion causes them to reach spin periods in the range 1–10 ms, faster than the spins they had at their formation. During that process, the magnetic field decreases from $\sim 10^{12}$ G to values near 10^8 G, which has the consequence of reducing the electromagnetic torque and contributes to their being more stable clocks than young RPPs. Such pulsars were first discovered in radio observations but (as described in Chapter [* *Wood* *]) in 1992 X-ray pulsations were discovered from some MSPs [3]. With their smaller magnetic fields, MSPs have not only lower period derivatives but also less timing noise. As a consequence, MSPs have far longer lifetimes than RPPs.

Overall, about a dozen of the known MSPs show X-ray pulses. These fall into two sub-classes. In one sub-class pulses are faint, soft, and broad but pulsars in this class are typically the best intrinsic clocks. In these cases the emission is thermal from a hot spot on the stellar surface with an effective temperature of about 2 keV. The other sub-class comprises MSPs that show bright, hard, narrow pulses and also exhibit a larger level of timing noise, or even rare glitches as in the case of PSR B1821–24 [4]. Notably, over 75 percent of all MSPs are in binary systems.

1.1 X-ray MSPs and Navigation

In a pulsar navigation system, measurements of pulse times of arrival (TOAs) are compared with predictions of those TOAs based on a timing model and the current estimate of the state vector (position and velocity) of the spacecraft. Measured differences between the measured and predicted TOAs are processed by an extended Kalman filter to derive an improved estimate of the spacecraft state vector. The performance of such a navigation system is determined by the precision of the TOA measurements and the accuracy of the timing model. Unlike a man-made satellite navigation system, the source location, brightness and modulation properties cannot be designed into the system. Yet, on long timescales (years) MSPs have noise

characteristics comparable to atomic clocks. The engineering challenge is to exploit the naturally-occurring MSPs to devise a practical navigation system. The long term stability of MSPs means that such a system can be highly autonomous, needing only very infrequent updates of the pulsar timing model parameters.

In this paper, we describe the properties of the specific pulsar sources and of the measurement system that together determine the accuracy of each TOA measurement and the prospects for increasing the catalog of useful pulsars. We also characterize the error budget for the timing model. Understanding the sources of error will allow for realistic expectations for the performance of pulsar-based navigation systems.

2 NICER/SEXTANT

While many points we will be making pertain to any pulsar navigation system, we illustrate them using the particular example of the SEXTANT technology demonstration that will be carried out using the NICER payload on the International Space Station (ISS). The performance goals for SEXTANT give an idea of what is feasible with current instruments on the ISS platform. The navigation accuracy requirement is 10 km in the worst of three directions, these being conventionally radial, in-track, and cross-track. This implies measuring pulsar arrival times to a typical accuracy of 33 μ s. The stretch goal is 1 km, or 3 μ s.

NICER is an X-ray timing experiment whose design has been highly optimized for millisecond pulsar observations [5]. It comprises 56 identical X-ray telescopes, each consisting of a concentrating X-ray optic and a single-pixel silicon drift detector (SDD). The complete payload has a mass of 263 kg and draws 337 W when in nominal operation. The peak total collecting area is over 1700 cm², about twice that of the XMM-Newton EPIC-pn camera, and it is sensitive to X-rays in the 0.2–12 keV band. A key feature for precise timing observations is that each photon is time-tagged to an accuracy of 100 ns (1σ) by reference to an onboard GPS receiver. NICER is scheduled to be launched in early 2017 and will be attached to the ISS for a minimum 24 month mission. Its primary science goals include constraining the dense matter equation-of-state by modeling the energy-dependent X-ray pulse profiles of millisecond pulsars, probing the rotational stability of MSPs, and searching for new periodic and quasi-periodic timing behavior from neutron star systems. It will also perform a wide variety of other observations that will be driven by an open-access guest observer program. The NICER instrument has been made as large as possible to provide high-quality science data. As such it is not a direct prototype of an avionics package for X-ray navigation, but results from navigation experiments can be scaled to packages of other sizes in other situations. In particular, for an interplanetary cruise where accelerations are small it would be feasible to do very long integrations, trading time for collecting aperture. This would permit avionics packages much smaller than NICER to be effective.

The SEXTANT team has developed a flight software application (called XFSW) that will run on the NICER flight processor [6, 7]. This application will enjoy on-board access to the X-ray photon data stream collected by the NICER X-ray timing instrument and can use that data stream to extract TOAs from particular pulsars as they are observed. The primary goal of the software application is to demonstrate, for the first time, the determination of the navigation solution for a spacecraft (in this case, the ISS) based solely on X-ray pulsar measurements onboard and in real time. This will be done during one or more intervals of two weeks each, during which the NICER observation schedule will be a sequence of MSPs optimized for navigation performance, rather than science. However, because much of the NICER science requires large amounts of observing time on MSPs, without imposing significant constraints on times when these data are collected, the SEXTANT-optimized observations will be fully useful for astrophysics as well.

3 TOA Measurement Accuracy

A TOA is a pulse arrival time, computed from a set of observed photon times recorded by a detector. The photon times are converted to pulse phases using a predictive model of the pulse period and are compared to a high signal-to-noise pulse template to determine the best estimate for the arrival time of a fiducial point on the template profile.

For binned data, this can be computed by finding the lag that maximizes the cross-correlation between a binned profile and the template. In fact, for binned data (as one might get from radio measurements or from very high photon count rates), a better method is to do the lag determination in the Fourier domain, taking advantage of the Fourier Shift Theorem, as described by [8].

For low-rate photon data, information is lost in the binning process and maximum likelihood methods are preferred [9, 10, 11]. Figure 1 illustrates the situation for low photon rates.

In either case, an algorithm running on the onboard processor determines the time of arrival, or TOA, of the pulse at the detector. In this section we describe the various contributions to the error budget for the TOA.

The first contribution to the TOA accuracy is the accuracy of the time stamp that provides the reference time for the TOA. As all measurements will be biased by any error in this time standard, this time must be accurate to better than the accuracy goal. For SEXTANT, the 100 ns accuracy provided by the NICER GPS time stamps is more than sufficient for even the stretch goal. Because time is referenced to GPS, for SEXTANT the pulsar measurements are used only for determining the position (and velocity) of the ISS. A future pulsar navigation system should be independent of GPS. This will require a stable local clock onboard, which the pulsar measurements would then steer to a pulsar-based time standard (akin to how GPS receivers steer their local oscillators to match GPS time). This will require more pulsars providing measurements to account for the additional dimension of the problem

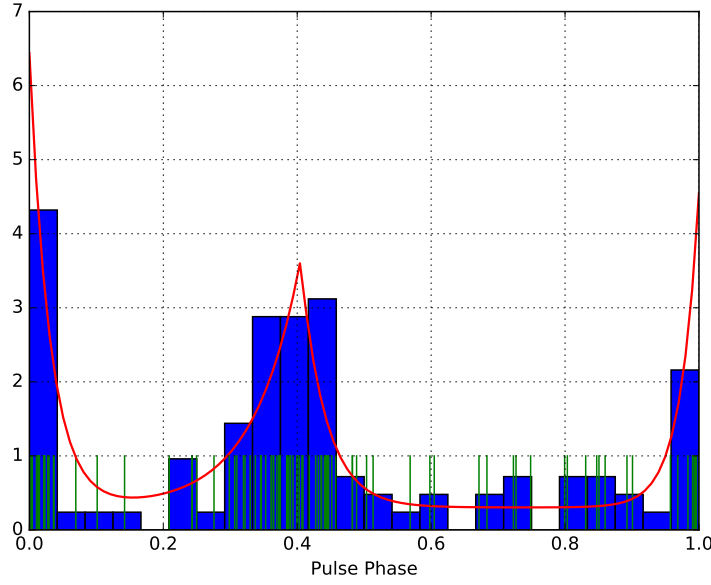


Fig. 1 The pulsar template (shown in red) approximates the ideal waveform that would be obtained in an extremely long integration. Actual integrations will have small numbers of photons (shown as green tick marks). Event times can be processed directly, or binned (blue histogram) for computational speed at some loss in time resolution.

(a minimum 4 pulsars, rather than 3). It will also set a stability requirement on the onboard clock. For example, we could set a requirement on the clock of $<3 \mu\text{s}$ drift over an interval long enough for at least 4 measurements to be processed (perhaps 10^3 seconds). This corresponds to a fractional frequency stability of 3×10^{-9} . To provide robustness in an actual system the required clock performance would probably need to be substantially better than this. It is worth noting that if the system is scaled down to a smaller detector then the interval required to collect measurements at a particular accuracy will grow and the requirements on the onboard clock stability will get more stringent.

Even with perfect time stamps, the accuracy of the arrival time will be determined by the noise statistics of the measured signal. The arrival times of the photons can be modeled as a non-homogeneous Poisson process (NHPP) with a rate function represented by the pulse template profile, designated by $h(\xi)$, where ξ is pulse phase in the range $[0, 1)$ and h is normalized such that $\int_0^1 h(\xi) d\xi = 1$. For a fully specified statistical model, the limiting performance of any estimator is set by the Cramér-Rao Lower Bound (CRLB), which yields the limiting or best accuracy in phase determination obtainable in a particular situation [12, 11].

Golshan & Sheikh (2007, eq. 24), derive the Cramér-Rao lower bound on the accuracy of an arrival time measurement (τ) as:

$$\sigma_\tau > \frac{P}{\sqrt{I_p T}}, \quad (1)$$

where P is the pulse period, T is the integration time, and

$$I_p = \int_0^1 \frac{(\alpha h'(\xi))^2}{\beta + \alpha h(\xi)} d\xi \quad (2)$$

The lower bound optimally exploits the pulse shape information in the light curve, in terms of $h(\xi)$ and its derivative $h'(\xi)$, and converts to measured results using coefficients α and β that characterize amplitudes of the signal and background in the detector system, respectively.

The values of I_p for the SEXTANT pulsars are listed in Table 1. These are numerically integrated from the template pulse profiles. In many cases, it is not convenient to compute these integrals and analytic approximations may be useful in certain limits. These also can assist in visualizing the scalings with the parameters. In the table below, we show the expressions for I_p in four cases, for purely gaussian or sinusoidal pulse profiles, and in the zero background ($\beta = 0$) case and the low signal case. Here, we define $\rho = \frac{\alpha}{\beta \sigma \sqrt{2\pi}}$. For the Gaussian low signal case, the expression is valid for $\rho < 1$ and the number of terms that need to be evaluated in the series gets smaller as ρ approaches 0.

	$h(\xi)$	$I_p(\beta = 0)$	$I_p(\beta \gg \alpha)$
Gaussian	$\frac{1}{\sigma\sqrt{2\pi}} e^{-(\xi-\xi_0)^2/2\sigma^2}$	α/σ^2	$\frac{\alpha}{\sigma^2} \rho \sum_{n=0}^{\infty} (n+2)^{-3/2} (-1)^n \rho^n$
Sinusoid	$1 - \cos(\xi)$	$(2\pi)^2 \alpha$	$\frac{\pi^2 \alpha^2}{2(\alpha + \beta)}$

The CRLB improves with cumulative integration time, T , as $1/\sqrt{T}$ for as long as Poisson statistics dominate the limit. In SEXTANT practice, it is not anticipated that one will integrate long enough for other error sources such as time stamp accuracy to become dominant. A rough rule of thumb for estimating the CRLB intuitively is that it equates to a characteristic width of the pulse divided by the signal-to-noise (SNR) expressed in standard deviations.

Figure 2 shows the simulated measurement uncertainty for several SEXTANT target pulsars vs. integration time, as compared to the CRLB. At long integration times, the measurement uncertainties approach the CRLB, as expected.

We note that the CRLB above is appropriate for situations where a single parameter is being determined (the pulse phase). If the uncertainty in the state vector is large enough and the orbit sufficiently dynamic (such as for the ISS in low Earth orbit), the measurement system may need to fit for multiple parameters (e.g. pulse phase and frequency, corresponding to a Doppler shift). In this case the CRLB on the TOA uncertainty is larger by a factor of two [11].

The CRLB depends on several factors including astrophysical issues intrinsic to the sources and particulars of the observing system. These factors influence the

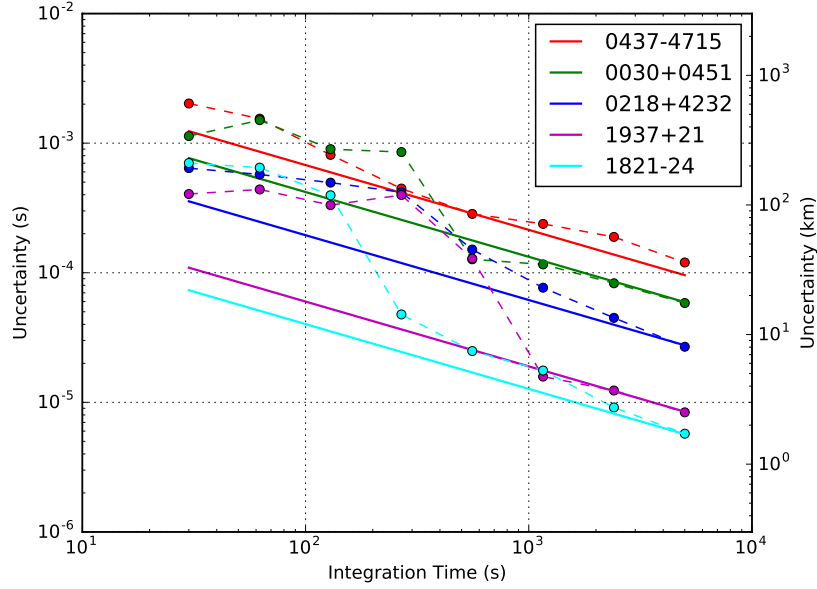


Fig. 2 Comparison of TOA accuracies (data points and dashed lines), based on event-by-event simulations and the actual SEXTANT measurement processing algorithm, for several SEXTANT target pulsars with the Cramér-Rao Lower Bound (CRLB, solid lines). At large integration times the measurement uncertainties approach the CRLB.

source selection and drive the optimal design of the instrument. We now examine them one by one.

3.1 Source count rate and its Estimation for Simulations

The measured count rate from a source depends on both the properties of the source (its flux and spectrum) and the detector system (its collecting area and quantum efficiency, as a function of energy). The pulsed X-ray emission from MSPs can be dominated either by thermal emission from the surface or by non-thermal emission from the magnetosphere [13]. In addition, the low-energy flux from the source can be absorbed by differing amounts of material along the line of sight. See Figure 3 for a comparison of several different MSP spectra. Thermal spectra with minimal absorption produce counts mostly in the 0.1–1 keV band, while non-thermal spectra, particularly those with significant absorbing columns, demand sensitivity extending out to several keV. For NICER, the effective area curve is included in the online

WebPIMMS¹ tool so count rates can be easily estimated for any specified source flux and spectrum. It should also be noted that once NICER is in orbit, it will become the best available instrument for determining both the X-ray spectra and pulsar light curves, and that the latter may turn out to vary with energy because of the varying blend of thermal and non-thermal components at different energies. This means that the initial models and templates used in SEXTANT may be refined as NICER progresses and replaced with versions of higher fidelity.

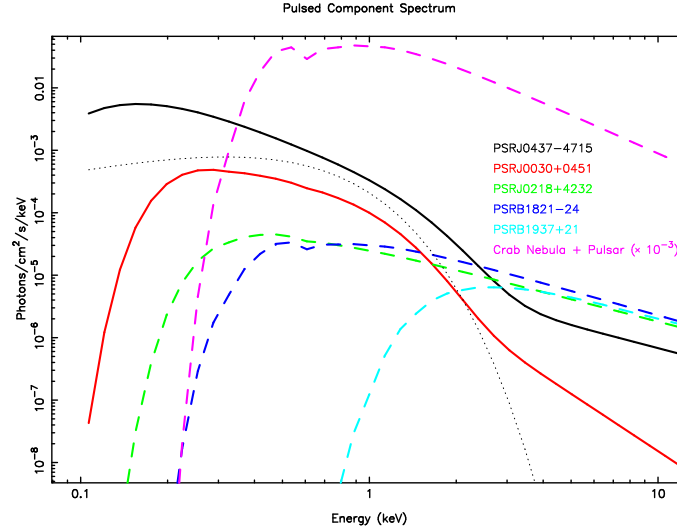


Fig. 3 X-ray spectra of several pulsars potentially useful for navigation applications. The thin dotted line is a 0.2 keV blackbody with no interstellar absorption, for comparison. Note that the magenta line is the Crab nebula and pulsar divided by 1000 to get it onto the same scale.

3.2 Background count rate

Unpulsed backgrounds from a variety of mechanisms contribute Poisson noise and reduce the accuracy of any TOA measurement.

A portion of the background is determined by the field of view of the instrument and the performance of the imaging or concentrating system. Any flux hitting the detector that comes from the diffuse X-ray background or any neighboring sources simply contributes to the background. These contributions can be reduced by a smaller field of view, at the expense of requiring a more precise instrument

¹ <http://heasarc.gsfc.nasa.gov/cgi-bin/Tools/w3pimms/w3pimms.pl>

pointing system. Similarly, any unpulsed flux from the pulsar source itself provides an irreducible background. For SEXTANT the diffuse X-ray background in the 3 arcmin FOV yields a background contribution of 0.15 counts/s.

In addition, particles or high energy photons that make it to the detector from other than the optical path can interact and create spurious events that contribute to the background. For NICER, this rate varies as the ISS moves in its orbit and encounters different trapped particle environments, as well as with solar activity. Another significant contribution to the radiation background for NICER comes from the Soyuz spacecraft docked at the ISS, whose γ -ray altimeters contain powerful radioactive sources. Together, these radiation backgrounds are estimated to contribute 0.05 counts/s to the NICER background rate.

Because the spectral shapes of most background components are different from the target pulsars, the performance can be optimized by making an energy selection that minimizes the CRLB for a source. In addition, if there are nearby sources making a significant background contribution, the instrument pointing can be offset to reduce that contribution. While the offset pointing reduces the signal from the source, in some cases it may reduce the background from the nearby contaminating source in a way that more than compensates.

3.3 Pulse Shapes

Finally, the CRLB is determined by the pulse shapes of the pulsars. All things being equal, pulse profiles with narrow features and steep gradients perform better than those with smooth, nearly-sinusoidal, profiles. However, it was noted earlier that there is an anti-correlation between sharp pulses and overall clock stability for actual MSPs. The pulse shape templates for six pulsars in the SEXTANT catalog are shown in Figure 4.

4 Source Catalog

The selection of sources for the SEXTANT catalog is driven by the performance requirements. SEXTANT's minimum performance requirement is being able to determine the ISS orbit to 10 km RMS (worst direction) by the end of a two-week experiment. The stretch performance goal is 1 km RMS. Since the speed of light is 300 m/ μ s, these location accuracies correspond to timing accuracies of 30 μ s and 3 μ s, respectively. TOA measurements (or model predictions) that are substantially worse than this contribute little to meeting the SEXTANT goals, although they may be useful in some circumstances such as in cold-start situations, or to resolve integer phase ambiguity issues with the primary MSPs. This provides a criterion for selecting individual sources to be included in the navigation catalog. However, the

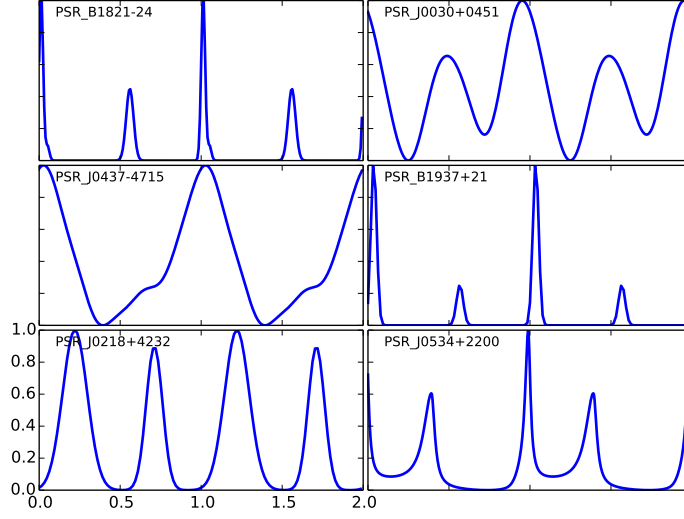


Fig. 4 Pulse profile templates for 6 of the SEXTANT target pulsars, showing the wide range in light curve shapes. For each pulsar two pulse cycles are displayed.

properties of the catalog as a whole also need to be considered when assessing system performance.

Table 1 SEXTANT Navigation Pulsar Catalog

PSR	P (ms)	α (c/s)	β (c/s)	I_p	σ_{CRLB} (μs)
Crab Pulsar	33.00	660.0	13860.2	56841.6	3.3
B1937+21	1.56	0.029	0.24	23.3	7.1
B1821-24	3.05	0.093	0.22	240.5	4.7
J0218+4232	2.32	0.082	0.20	5.6	22.9
J0030+0451	4.87	0.193	0.20	5.4	49.3
J1012+5307	5.26	0.046	0.20	0.5	168.6
J0437-4715	5.76	0.283	0.62	2.9	79.7
B1509-58	151.25	6.5	0.20	347.8	191.2

Table 1 shows the primary catalog of navigation sources currently being used for SEXTANT. The pulse period, source (α) and background (β) counting rates expected in NICER, I_p , and the CRLB estimate for the TOA uncertainty in an 1800 s measurement are included. Note that the Crab pulsar is much brighter than the others and has a high α but also a high β that mostly comes from the off-pulse emission of the pulsar and its surrounding nebula. For most of the other sources β is about 0.2 c/s, but J0437-4715 has a higher rate because of the contaminating influence of a nearby source.

Figure 5 shows the distribution on the sky of the pulsars used by SEXTANT. The pulsars do not concentrate preferentially along the Galactic plane because of the large scale height of the millisecond pulsar population and the fact that most X-ray detected MSPs are relatively nearby. Thus they are a nearly isotropic population, providing a good geometry for navigation.

Source visibility constraints limit when each source can be observed. There are exclusions for Sun, Moon, Earth blockage, and ISS structure blockage. In the figure, the solar exclusion zone is a moving circle centered on the horizontal axis, which is the Ecliptic plane.

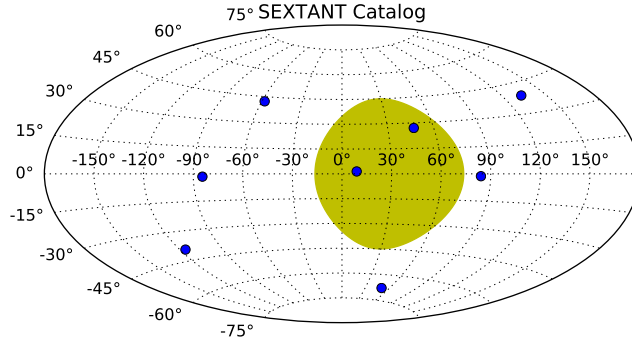


Fig. 5 Sky map in ecliptic coordinates, showing the pulsars in the SEXTANT catalog. The shaded region represents the solar exclusion region (shown here at one instant in time), which moves horizontally on the map over the course of a year.

The source catalog in Table 1 may also change as new pulsars are discovered and characterized. Many new candidates are being found using the *Fermi Gamma-ray Space Telescope* and in follow-ups with ground-based radio observations. In addition, NICER itself is expected to detect new X-ray pulsations from several millisecond pulsars as part of its science program. As these pulsars are discovered and characterized they are assessed for their navigational potential.

5 Model Accuracy

Any error in the prediction of when a pulse should arrive directly translates into an error in the derived navigation solution. The timing models used to generate the predictions must be maintained by a program of radio, X-ray, or γ -ray observations, informed by the best current understanding of astrophysical mechanisms at work in the sources. Typically the highest precision TOAs are obtained from radio observations, but care must be taken to account for variable propagation effects that affect

radio observations, but not X-ray observations (which are effectively at infinite frequency).

A useful source of timing information comes from pulsar timing array programs, designed to detect gravitational waves. (In principle, gravitational waves make additional minute contributions to the phase errors in received pulses.) Currently the NANOGrav project [14] is timing several of the SEXTANT pulsars, and the Nançay observatory in France has a long-term timing program on several others (some overlapping), importantly including the source B1821–24. The SEXTANT team has signed Memoranda of Understanding with both of those groups, providing for sharing of the timing data for X-ray navigation purposes. In addition, several of the pulsars are observed continuously in γ -rays by *Fermi* [15]. Jodrell Bank observes the Crab pulsar daily² and the Parkes Pulsar Timing Array (PPTA) monitors 20 pulsar, including the important PSR J0437–4715 [16]. After launch, NICER itself will be an excellent source of precision timing information for the SEXTANT pulsars.

These data are used to derive parameterized timing models that predict the arrival of any individual pulse to high precision, typically using a pulsar timing code like TEMPO2 [17]. Many of these parameters are deterministic, meaning that they are a measurement of a physical property of the system (e.g. spin frequency, position, proper motion, binary system parameters) that can be used to predict TOAs forward in time with uncertainty bounded by the uncertainty in the determination of the model parameters. However, there are some effects that are not stationary, or are stochastic. When these are present, the accuracy of the predictions will degrade with time, regardless of the precision with which the model parameters are determined from the current data. Fortunately, these effects are rather small for MSPs. We discuss some of them below.

5.1 DM variations

The dispersion measure (DM) characterizes how the radio pulse is delayed as a function of frequency caused by the frequency dependence of the group velocity of a radio wave traveling in the tenuous plasma of interstellar space. The time delay relative to a signal of infinite frequency is [18]

$$\Delta t = \mathcal{D} \times \frac{DM}{f^2} \quad (3)$$

where $\mathcal{D} = 4148.8 \text{ MHz}^2 \text{ pc}^{-1} \text{ cm}^3 \text{ s}$, and f is the observing frequency. If the DM were constant there would be a constant correction between the radio pulse arrival time (at a particular frequency) and that in X-rays. In principle this delay can be measured and removed by making timing observations at two or more radio frequencies. However, variations in the column density of free electrons as the line of sight moves through the complex and turbulent interstellar medium cause stochastic

² <http://www.jb.man.ac.uk/pulsar/crab.html>

wandering of the DM that is not predictable over long time scales. The DM variation versus time for several SEXTANT pulsars is shown in Figure 6.

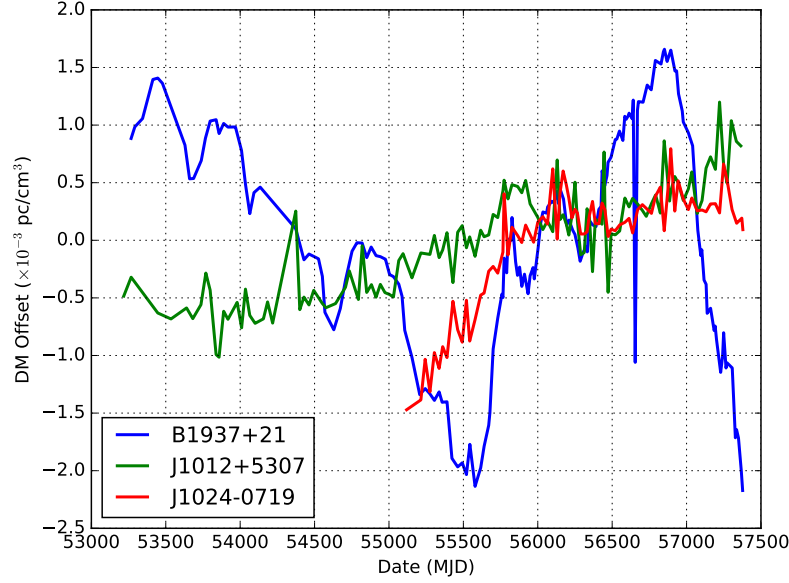


Fig. 6 Dispersion Measure (DM) variations can produce errors in extrapolation from radio data to the X-ray band. These data are from NANOGrav timing measurements [19]. For reference, the time offset caused by a DM error of $1.0 \times 10^{-3} \text{ pc cm}^{-3}$ from 1400 MHz to infinite frequency is $2 \mu\text{s}$.

5.2 Red noise and model extrapolation

In addition to unpredictable DM variations, some MSPs exhibit red noise akin to the timing noise seen in young RPPs. This is modeled as a stochastic process with a steep spectrum. As an example, in an analysis of 9 years of NANOGrav timing data, red noise was detected in 10 out of 37 MSPs. This red noise causes the arrival times to drift relative to the deterministic model by a few microseconds over timescales of a few years.

Care must be taken when extrapolating timing models for pulsars with significant red noise contributions. If the red noise is modeled using a high order polynomial, it will extrapolate very poorly and the predictions will diverge from the true arrival times very quickly. A better method is to construct an optimal extrapolation based

on the statistical properties (i.e. the covariance matrix) of the red noise [20]. This method is implemented in the `interpolate` plugin for TEMPO2.

The Crab pulsar is an important special case. Unlike the other SEXTANT sources it is a young, bright RPP and not a MSP. It is much brighter than the MSPs, so can be detected in a far shorter observation, yet has much more timing noise. Over short intervals and with good support from ground observations it can be an important contributor to navigation performance, particularly in a highly dynamic situation (such as an orbital maneuver). To maintain prediction accuracies of $10 \mu\text{s}$, ephemeris updates are needed roughly every three days when the Crab is being employed for navigation. Figure 10 shows period excursions for the Crab over an interval of a month and also illustrates the impracticality of trying to extrapolate outside the observed interval.

For MSPs, the parameters are known well enough, and the effects of red noise and DM variations are small enough, that a timing model can predict phase to the accuracy required for SEXTANT for months into the future.

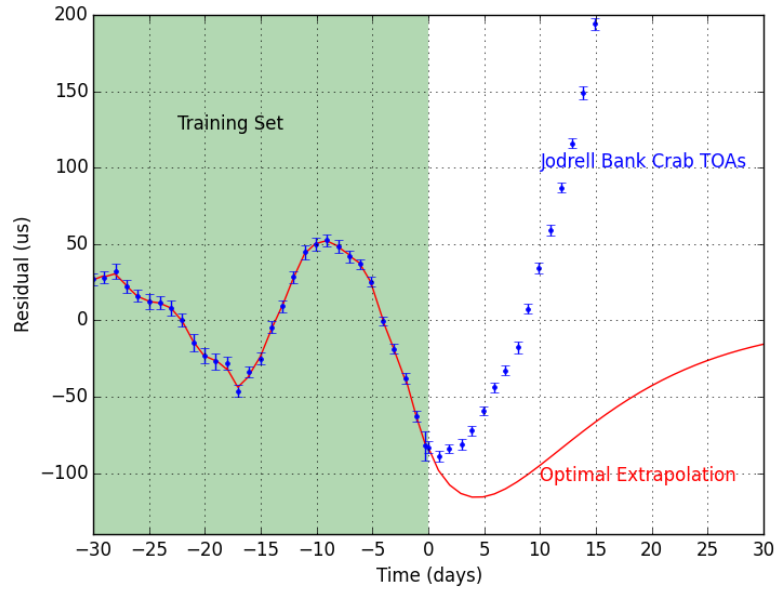


Fig. 7 The growth of residuals with days elapsed since the end of measurements, for the Crab pulsar. The model was fit to the data in the green region, and the red curve shows the optimal extrapolation into the future. The actual arrival times (blue points) diverge from the extrapolation rather quickly, so for navigational purposes and the Crab timing model must be updated frequently throughout the interval of use. MSPs, however, are much less noisy and for them extrapolations beyond the fitted interval are viable for far longer.

6 Conclusion

Pulsar navigation has been discussed for some years as a natural analog to global navigation satellite systems (GNSS) that may have important applications in cases of GNSS unavailability or for missions that travel deep into interplanetary or interstellar space [21].

As we have shown, the performance of such a system depends on the properties of the pulsars and measurement system, as well as the ability of the pulsar timing models to predict pulse arrival times into the future.

The SEXTANT demonstration using the NICER X-ray timing instrument will be a major milestone in the development of X-ray navigation. The SEXTANT results will inform the development of realistic navigation instruments based on X-ray pulsar observations. In addition, NICER should discover several new X-ray millisecond pulsars that can contribute to navigation applications.

Acknowledgements SEXTANT work at NRL is supported by NASA NPR NNG13LM70I.

References

1. S.I. Sheikh, D.J. Pines, K.S. Wood, P.S. Ray, M.N. Lovellette, M.T. Wolff, *Journal of Guidance, Control, and Dynamics* **29**(1), 49 (2006)
2. Z. Arzoumanian, D.J. Nice, J.H. Taylor, S.E. Thorsett, *ApJ* **422**, 671 (1994). DOI 10.1086/173760
3. W. Becker, J. Trümper, *Nature* **365**, 528 (1993). DOI 10.1038/365528a0
4. I. Cognard, D.C. Backer, *ApJ* **612**, L125 (2004). DOI 10.1086/424692
5. Z. Arzoumanian, K.C. Gendreau, C.L. Baker, T. Cazeau, P. Hestnes, J.W. Kellogg, S.J. Kenyon, R.P. Kozon, K.C. Liu, S.S. Manthripragada, C.B. Markwardt, A.L. Mitchell, J.W. Mitchell, C.A. Monroe, T. Okajima, S.E. Pollard, D.F. Powers, B.J. Savadkin, L.B. Winternitz, P.T. Chen, M.R. Wright, R. Foster, G. Prigozhin, R. Remillard, J. Doty, in *Astronomical Telescopes and Instrumentation, Proc. SPIE*, vol. 9144 (International Society for Optics and Photonics, 2014), *Proc. SPIE*, vol. 9144, pp. 914,420–914,420–9. DOI 10.1117/12.2056811. URL <http://dx.doi.org/10.1117/12.2056811>
6. J.W. Mitchell, M.A. Hassouneh, L.B. Winternitz, J.E. Valdez, P.S. Ray, Z. Arzoumanian, K.C. Gendreau, in *Proceedings of the 27th International Technical Meeting of the Satellite Division of the Institute of Navigation (ION GNSS+)* (Institute of Navigation, 2014)
7. J.W. Mitchell, M.A. Hassouneh, L.M. Winternitz, J.E. Valdez, S.R. Price, S.R. Semper, W.H. Yu, Z. Arzoumanian, P.S. Ray, K.S. Wood, R.J. Litchford, K.C. Gendreau, in *AIAA Guidance, Navigation, and Control Conference*, AIAA SciTech (American Institute of Aeronautics and Astronautics, 2015). URL <http://dx.doi.org/10.2514/6.2015-0865>
8. J.H. Taylor, *Philosophical Transactions of the Royal Society of London Series A* **341**, 117 (1992). DOI 10.1098/rsta.1992.0088
9. P.S. Ray, M. Kerr, D. Parent, A.A. Abdo, L. Guillemot, S.M. Ransom, N. Rea, M.T. Wolff, A. Makeev, M.S.E. Roberts, F. Camilo, M. Dormody, P.C.C. Freire, J.E. Grove, C. Gwon, A.K. Harding, S. Johnston, M. Keith, M. Kramer, P.F. Michelson, R.W. Romani, P.M. Saz Parkinson, D.J. Thompson, P. Weltevrede, K.S. Wood, M. Ziegler, *ApJS* **194**, 17 (2011). DOI 10.1088/0067-0049/194/2/17
10. M.A. Livingstone, S.M. Ransom, F. Camilo, V.M. Kaspi, A.G. Lyne, M. Kramer, I.H. Stairs, *ApJ* **706**, 1163 (2009). DOI 10.1088/0004-637X/706/2/1163

11. L. Winternitz, M. Hassouneh, J. Mitchell, J. Valdez, S. Price, S. Semper, W. Yu, P. Ray, K. Wood, Z. Arzoumanian, K. Gendreau, in *Aerospace Conference, 2015 IEEE* (IEEE, 2015). DOI 10.1109/AERO.2015.7118936. URL <http://dx.doi.org/10.1109/AERO.2015.7118936>
12. A.R. Golshan, S.I. Sheikh, in *Proceedings of the 63rd Annual Meeting of The Institute of Navigation* (Institute of Navigation, Cambridge, MA, 2007), pp. 413–422
13. V.E. Zavlin, *ApSS* **308**, 297 (2007). DOI 10.1007/s10509-007-9297-y
14. M.A. McLaughlin, *Classical and Quantum Gravity* **30**(22), 224008 (2013). DOI 10.1088/0264-9381/30/22/224008
15. M. Kerr, P.S. Ray, S. Johnston, R.M. Shannon, F. Camilo, *ApJ* **814**, 128 (2015). DOI 10.1088/0004-637X/814/2/128
16. D.J. Reardon, G. Hobbs, W. Coles, Y. Levin, M.J. Keith, M. Bailes, N.D.R. Bhat, S. Burke-Spolaor, S. Dai, M. Kerr, P.D. Lasky, R.N. Manchester, S. Osłowski, V. Ravi, R.M. Shannon, W. van Straten, L. Toomey, J. Wang, L. Wen, X.P. You, X.J. Zhu, *MNRAS* **455**, 1751 (2016). DOI 10.1093/mnras/stv2395
17. G.B. Hobbs, R.T. Edwards, R.N. Manchester, *Monthly Notices of the Royal Astronomical Society* **369**, 655 (2006). DOI 10.1111/j.1365-2966.2006.10302.x. URL <http://adsabs.harvard.edu/abs/2006MNRAS.369..655H>
18. D. Lorimer, M. Kramer, *Handbook of Pulsar Astronomy* (Cambridge University Press, 2005)
19. The NANOGrav Collaboration, Z. Arzoumanian, A. Brazier, S. Burke-Spolaor, S. Chamberlin, S. Chatterjee, B. Christy, J.M. Cordes, N. Cornish, K. Crowter, P.B. Demorest, T. Dolch, J.A. Ellis, R.D. Ferdman, E. Fonseca, N. Garver-Daniels, M.E. Gonzalez, F.A. Jenet, G. Jones, M.L. Jones, V.M. Kaspi, M. Koop, M.T. Lam, T.J.W. Lazio, L. Levin, A.N. Lommen, D.R. Lorimer, J. Luo, R.S. Lynch, D. Madison, M.A. McLaughlin, S.T. McWilliams, D.J. Nice, N. Palliyaguru, T.T. Pennucci, S.M. Ransom, X. Siemens, I.H. Stairs, D.R. Stinebring, K. Stovall, J.K. Swiggum, M. Vallisneri, R. van Haasteren, Y. Wang, W. Zhu, *ApJ* **813**, 65 (2015). DOI 10.1088/0004-637X/813/1/65
20. X.P. Deng, W. Coles, G. Hobbs, M.J. Keith, R.N. Manchester, R.M. Shannon, J.H. Zheng, *MNRAS* **424**, 244 (2012). DOI 10.1111/j.1365-2966.2012.21189.x
21. S. Sheikh, D. Pines, K.S. Wood, P.S. Ray, M.N. Lovellette. Navigational system and method utilizing sources of pulsed celestial radiation (2007). URL <https://www.google.com/patents/US7197381>. U.S. Patent 7,197,381